Structural Evolution of Layered $Li_xMn_yO_2$: Combined Neutron, NMR, and Electrochemical Study

A. Robert Armstrong,† Allan J. Paterson,† Nicolas Dupré,‡ Clare P. Grey,‡ and Peter G. Bruce*,†

School of Chemistry, The Purdie Building, University of St Andrews, Fife, KY16 9ST, United Kingdom, and Chemistry Department, State University of New York at Stony Brook, Stony Brook, New York 11794-3400

Received September 12, 2006. Revised Manuscript Received December 8, 2006

The conversion upon electrochemical cycling from a layered structure to a spinel in nonstoichiometric $Li_xMn_yO_2$ has been studied by neutron diffraction and NMR. This process occurs in all layered lithium manganate materials, irrespective of the ion-exchange route. The high temperature of the ion exchange under reflux in *n*-hexanol is sufficient to promote formation of some spinel within the as-synthesized material. Upon cycling, all the different layered $Li_xMn_yO_2$ compounds begin to transform to a spinel. In the first 50 or so cycles, the various layered $Li_xMn_yO_2$ compounds behave rather differently, with a higher spinel fraction being observed for materials ion-exchanged under more extreme conditions. However, the rate of this transformation is significantly slower than was observed in stoichiometric layered $LiMnO_2$, with only 25% spinel observed after 100 cycles. Ultimately, upon extended cycling, the entire structure will form a well-ordered spinel phase.

Introduction

We recently reported on the structural evolution of the stoichiometric form of layered $LiMnO_2$ upon extended electrochemical cycling from a layered compound to a spinel.[1] While structural transformations such as this are themselves interesting, they may also have important consequences for the properties, and thus applications, of such materials in devices like rechargeable lithium batteries.[2,3] The synthesis of layered $LiMnO_2$ was first reported several years ago.[4,5] Following the initial discovery it was demonstrated that the material may be prepared as both stoichiometric $LiMnO_2$ and nonstoichiometric $Li_xMn_yO_2$ ($x \sim 0.6$, $y \sim 0.95$).[6−8] Interest in these layered lithium manganese oxides, both unsubstituted and those in which some of the Mn is replaced by other ions, arises because of their low cost, low toxicity, and high capacity (200 $mA{\cdot}h{\cdot}g^{-1}$ at a rate of 25 $mA{\cdot}g^{-1}$) when used as positive electrodes in rechargeable lithium batteries.[9−14] Although the nonstoichiometric materials transform to spinel, they do so with remarkably little influence on the variation in capacity with cycle number because of the nanodomain structure of the resulting spinel.[6,8,10] The structures of layered lithium manganese oxides may be described as cubic close-packed oxide ion layers stacked in an ABC sequence with alternate sheets of octahedral sites between the layers being occupied by Li and Mn (the sites are fully occupied in the case of stoichiometric $LiMnO_2$ but exhibit vacancies in the Li and Mn sites for the nonstoichiometric materials).[8]

In our previous study on the structural evolution of stoichiometric layered $LiMnO_2$ upon electrochemical cycling, we used solid-state NMR and powder neutron diffraction as probes, combined with electrochemical measurements.[1] It is important to monitor the structural changes with techniques that probe both short and long-range structure. Magic-angle spinning (MAS) NMR was chosen as a probe of the local structure. Extensive investigations of Li NMR in lithium manganese oxide compounds has enabled the shifts expected for various lithium environments in these materials to be determined.[15,16] Since Li is a weak scatterer of X-rays, it is advantageous to employ neutron powder diffraction for the

* Corresponding author: e-mail pgb1@st-andrews.ac.uk.
† University of St Andrews.
‡ SUNY Stony Brook.

(1) Armstrong, A. R.; Paterson, A. J.; Dupre, N.; Grey, C. P.; Bruce, P. G. *Chem. Mater.* **2004**, *16*, 3106.
(2) Bruce, P. G.; Irvine, J. T. S. In *Encyclopedia of Materials: Science and Technology*; Elsevier: Oxford, U.K., 2002.
(3) Tarascon, J.-M.; Armand, M. *Nature* **2001**, *414*, 359.
(4) Armstrong, A. R.; Bruce, P. G. *Nature* **1996**, *381*, 499.
(5) Capitaine, F.; Gravereau, P.; Delmas, C. *Solid State Ionics* **1996**, *89*, 197.
(6) Armstrong, A. R.; Gitzendanner, R.; Robertson, A. D.; Bruce, P. G. *Chem. Commun.* **1998**, *1833*.
(7) Robertson, A. D.; Armstrong, A. R.; Bruce, P. G. *Chem. Commun.* **2000**, *1997*.
(8) Armstrong, A. R.; Paterson, A. J.; Robertson, A. D.; Bruce, P. G. *Chem. Mater.* **2002**, *14*, 710.
(9) Armstrong, A. R.; Robertson, A. D.; Gitzendanner, R.; Bruce, P. G. *J. Solid State Chem.* **1999**, *145*, 549.
(10) Robertson, A. D.; Armstrong, A. R.; Fowkes, A. J.; Bruce, P. G. *J. Mater. Chem.* **2001**, *11*, 113.
(11) Quine, T. E.; Duncan, M. J.; Armstrong, A. R.; Robertson.; A. D.; Bruce, P. G. *J. Mater. Chem.* **2000**, *10*, 2838.
(12) Robertson, A. D.; Armstrong, A. R.; Paterson, A. J.; Duncan, M. J.; Bruce, P. G. *J. Mater. Chem.* **2003**, *13*, 2367.
(13) Ammundsen, B.; Desilvestro, J.; Groutso, T.; Hassell, D.; Metson, J. B.; Regan, E.; Steiner, R.; Pickering, P. J. *J. Electrochem. Soc.* **2000**, *147*, 4078.
(14) Davidson, I. J.; McMillan, R. S.; Slegr, H.; Luan, B.; Kargina, I.; Murray, J. J.; Swainson, I. P. *J. Power Sources* **1999**, *81−82*, 406.
(15) Lee, Y. J.; Wang, F.; Grey, C. P. *J. Am. Chem. Soc.* **1998**, *120*, 12601
(16) Lee, Y. J.; Wang, F.; Mukerjee, S.; McBreen, J.; Grey, C. P. *J. Electrochem. Soc.* **2000**, *147*, 803.

10.1021/cm0621747 CCC: $37.00
Published on Web 02/09/2007

investigation of long-range structure in lithium compounds. Until recently this has required sample sizes of at least 0.5−1 g. Although it is possible to cycle electrochemical cells with electrodes of this size, it is not feasible to achieve high cycle numbers at comparable rates, and thus similar time scales, to those of smaller cells. The advent of high-intensity neutron powder diffractometers with high detector area, such as GEM at the ISIS facility, Rutherford Appleton Laboratory, represented a significant breakthrough in the study of intercalation electrodes. It is now possible to obtain high-quality neutron powder diffraction data on samples of around 50 mg in a few hours. We have made extensive use of this instrument in the course of the present work.

In the stoichiometric system we observed a gradual transformation from layered $LiMnO_2$ to the spinel structure. Upon first extracting Li from $LiMnO_2$, Jahn−Teller-inactive Mn^{4+} forms. As a result of the rapid mobility of Li^+ and e^-, segregation into regions of undistorted $Li_{0.5}MnO_2$ of $R\bar{3}m$ symmetry and regions of Jahn−Teller-distorted $LiMnO_2$ of $C2/m$ symmetry provides an energetically feasible way of accommodating the mixture of Jahn−Teller-active Mn^{3+} and inactive Mn^{4+}. The two phases coexist within the composition range $Li_{0.5}MnO_2$ to $LiMnO_2$. Once $Li_{0.5}MnO_2$ forms, Mn ions can migrate from the octahedral sites in the transition metal layers through a shared face into an empty tetrahedral site located in the Li layers. The Li ions in the alkali metal layers will avoid the three octahedral sites that share faces with this tetrahedral site in order to minimize repulsions. The displacement of these Mn ions also makes it possible for Li to move from the octahedral to tetrahedral sites within the Li layers, to form the so-called "Li−Mn" dumbbells that were proposed in an earlier density functional theory (DFT) study of this layered-to-spinel transformation.[17] This was previously impossible since such sites shared faces with the octahedrally coordinated Mn ions in the transition metal layers. As a result of these changes, we observe Li/Mn ions in tetrahedral sites within a layered structure; that is, formation of a so-called "splayered" phase. Subsequent cycling reveals that this splayered phase persists and does not change substantially in composition but gradually transforms to spinel. However, it appears that this transformation occurs through an intermediate, with many features common to spinel, as probed by NMR, but with a long-range structure that can still be described by using the splayered structural model. The proportion of Li ions in these intermediate environments grows up to cycle number 25. As cycling continues, long-range ordered spinel forms and is evident in the diffraction and NMR data. Ultimately, upon extended cycling the entire structure forms a relatively well-ordered crystalline spinel phase.

In the present paper we examine the structural evolution of a range of nonstoichiometric $Li_xMn_yO_2$ materials upon electrochemical cycling. In this system the values of x and y are dependent upon the conditions employed in the ion exchange from the corresponding sodium phase. As a result we have examined the behavior of materials prepared in a number of different ways to explore the effect that nonstoichiometry plays in controlling structural evolution.

Experimental Section

Nonstoichiometric $Na_xMn_yO_2$ was prepared by mixing Na_2CO_3 (Aldrich, 99.5+%) and $Mn(CH_3CO_2)_2{\cdot}4H_2O$ (Aldrich, 99+%) in distilled water in stoichiometric ratios corresponding to $x/y = 0.67$. After rotary evaporation, the mixture was heated in air at 250 °C for 12 h to decompose the acetates. The resulting powder was fired at 600 °C in air for 1 h followed by quenching. The sodium phase was then ion-exchanged under a range of conditions. The most extreme conditions involved refluxing in *n*-hexanol at 160 °C with a 7−8-fold molar excess of LiBr for up to 8 h. Other conditions involved refluxing in *n*-butanol (120 °C) and refluxing in ethanol (80 °C). These milder ion-exchange conditions required longer times to achieve completion. The resulting materials were washed with ethanol and dried overnight. Chemical analyses for sodium and lithium were carried out by flame emission;analysis for manganese was by atomic absorption spectroscopy. The average manganese oxidation state was determined by redox titration with ferrous ammonium sulfate/$KMnO_4$.[18] Powder X-ray diffraction data were collected on a Stoe STADI/P diffractometer operating in transmission mode with Fe $K\alpha_1$ radiation ($\lambda = 1.936$ Å) to eliminate Mn fluorescence.

In order to prepare the electrochemically cycled materials for characterization by neutron diffraction and solid-state NMR, composite electrodes were constructed by mixing the active material, carbon, and Kynar Flex 2801 [a copolymer based on poly(vinylidene difluoride), PVDF] in the weight ratios 85:10:5. The mixture was prepared as a slurry in tetrahydrofuran (THF) and spread onto aluminum foil by a Doctor Blade technique. Following evaporation of the solvent and drying, electrodes were incorporated into an electrochemical cell with a lithium metal counterelectrode and the electrolyte was a 1 *m* solution of $LiPF_6$ in ethylene carbonate/dimethyl carbonate (1:1) (Merck). Electrochemical measurements were carried out on a Biologic MacPile II. Typically cells were cycled between 2.5 and 4.6 V at rates of around 25 $mA{\cdot}g^{-1}$. After cycling, the Kynar was dissolved and the samples were centrifuged before drying and loading into 2 mm quartz capillaries for neutron diffraction measurements.

An additional series of samples was prepared for the ^{6}Li NMR experiments. The ion exchange was performed with ^{6}LiCl instead of LiBr, and ^{6}Li-enriched Li metal was used as the anode in the electrochemical measurements. An aluminum disk was coated with a slurry, made by adding cyclopentanone to a mixture composed of 80% active material and 20% acetylene black carbon, and the disk was dried under vacuum at ambient temperature for a few hours. A 1 *m* $LiPF_6$ solution in ethylene carbonate/dimethyl carbonate (1:1, Merck) was used as electrolyte. The cells were assembled in an argon atmosphere. Samples were stabilized electrochemically, after galvanostatic cycling, by use of the potentiodynamic mode with Li metal as the negative and reference electrode. Samples were equilibrated at potentials corresponding to different steps of the intercalation/deintercalation process. A range of potentials was chosen so that all major processes were monitored. The cells were then disassembled and the cathodes were washed with ethylene carbonate/dimethyl carbonate (EC/DMC) to remove residual electrolyte, before the samples were packed in NMR rotors in an inert atmosphere for the NMR experiments.

Time-of-flight powder neutron diffraction data on the cycled materials were obtained on the GEM diffractometer at ISIS at the

(17) Reed, J.; Ceder, G.; van der Ven, A. *Electrochem. Solid-State Lett.* **2001**, *4*, A78.

(18) Katz, M. J.; Clarke, R. C.; Nye, W. F. *Anal. Chem.* **1956**, *28*, 507.

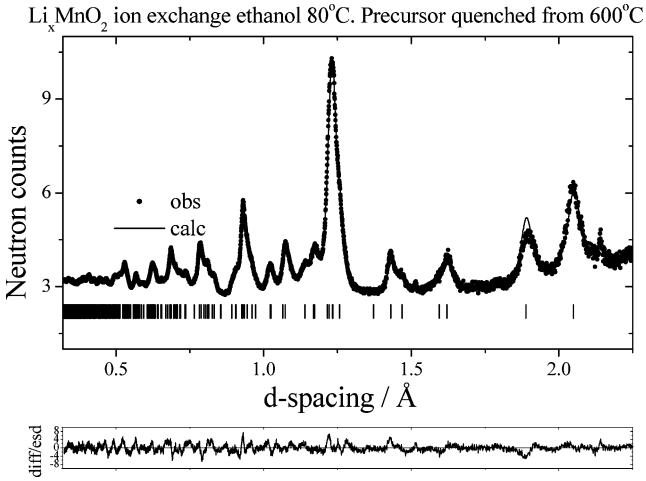

Figure 1. Refined powder neutron diffraction pattern for as-synthesized layered $Li_xMn_yO_2$ prepared by ion exchange under reflux in ethanol. (●) observed data; (—) calculated pattern. The lower line is the difference/esd.

Table 1. $Li_xMn_yO_2$ Chemical Analysis Results[a]

preparative conditions	calcd composition	avg Mn oxidation state
(600 °C Q); ethanol, 80 °C	$Na_{0.069}Li_{0.59}Mn_{0.94}O_2$	3.55+
(600 °C Q); butanol, 120 °C	$Na_{0.056}Li_{0.77}Mn_{0.91}O_2$	3.49+
(600 °C Q); hexanol, 160 °C	$Na_{0.035}Li_{0.61}Mn_{1.01}O_2$	3.32+

[a] Parentheses indicate conditions for Na-phase synthesis; Q = quenched.

Rutherford Appleton Laboratory. The samples were contained in 2 mm quartz capillaries. The structures were refined by the Rietveld method using the program Prodd based on the Cambridge Crystallographic Subroutine Library (CCSL).[19,20] Scattering lengths of −0.19, −0.373, and 0.5803 (all × 10^{-12} cm) were assigned to Li, Mn, and O, respectively.[21]

The cathode materials were probed by ^{6}Li magic-angle spinning (MAS) NMR spectroscopy, since higher resolution spectra may be typically obtained from this nucleus compared to ^{7}Li MAS NMR. First, the ^{6}Li MAS NMR experiments were run on the same samples used in the diffraction experiments. However, in order to increase the signal-to-noise ratio and to allow weaker peaks to be detected, the ^{6}Li NMR spectra shown here were acquired from cathode materials cycled with ^{6}Li-enriched Li anode. Other than the signal-to-noise ratio, the ^{6}Li spectra of these samples were identical to those prepared for the neutron experiments; these spectra are presented in this paper. Moreover, the samples cycled against the ^{6}Li anode displayed similar electrochemical behavior to their natural-abundance Li counterparts, ensuring a study of rigorously equivalent samples by both ^{6}Li NMR and neutron diffraction. Experiments were performed at an operating frequency of 29.47 MHz on a CMX-200 spectrometer. Spinning frequencies of 35 kHz were achieved by use of a fast MAS 2 mm probe, built by A. Samoson and co-workers. All spectra were acquired with a rotor-synchronized echo sequence (90°-τ-180°-τ-acq), where $\tau = 1/\nu_r$. A $\pi/2$ pulse width of 2.8 μs for ^{6}Li on the CMX-200 spectrometer was used with a pulse delay of 0.2 s. "Room temperature" (i.e., a spectrum acquired with no control of the temperature) corresponds typically to a sample temperature of between 70 and 80 °C.

(19) Matthewman, J. C.; Thompson, P.; Brown, P. J. *J. Appl. Crystallogr.* **1982**, *15*, 167.
(20) Brown, P. J.; Matthewman, J. C. Report RAL-87-010; Rutherford Appleton Laboratory: Oxfordshire, U.K., 1987.
(21) Sears, V. F. *Neutron News* **1992**, *3* (3), 26.

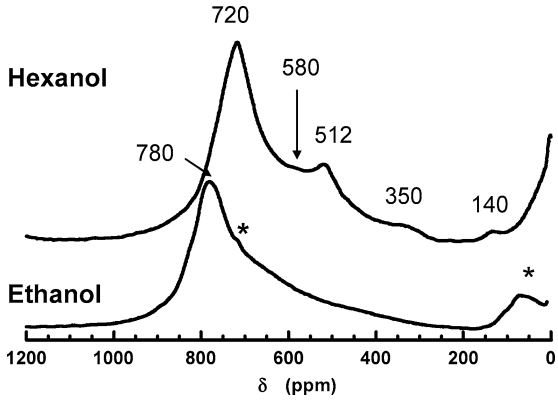

Figure 2. Comparison of the ^{6}Li MAS NMR spectra of samples prepared in hexanol vs ethanol. The intense resonance at 0 ppm is due to lithium salts in the electrolyte.

Results

The as-prepared $Li_xMn_yO_2$ materials adopt the *O*3 structure. Powder neutron diffraction data were refined by use of a rhombohedral layered model in space group $R\bar{3}m$, as has been reported previously.[8] A fitted neutron powder diffraction pattern for layered $Li_xMn_yO_2$ prepared by ion exchange under reflux in ethanol is shown in Figure 1. The structure consists of close-packed oxide ion layers stacked in an ABC sequence with alternate sheets of octahedral sites occupied by Li and Mn. The structure is essentially that of $LiCoO_2$ (α-$NaFeO_2$ type) but with cation vacancies on both the Li (3b) and Mn (3a) sites. Some residual sodium is found on the 3b sites. The Jahn−Teller-active high-spin $3d^4$ Mn^{3+} ion is present at sufficiently low concentration that there is no structural distortion. Lattice parameters obtained from the refinement were $a = 2.8608(3)$ and $c = 14.5877(18)$ Å, with *R*-factors $R_e = 1.0\%$, $R_{wP} = 2.1\%$, and $R_P = 3.4\%$. The amount of residual sodium and concentration of vacancies on the transition metal sites both decrease with increasing ion-exchange temperature, that is, upon changing the solvent used in the ion-exchange from ethanol to butanol to hexanol, as shown in Table 1.[8]

The ^{6}Li MAS NMR spectrum of the same material is consistent with this structural model but indicates the presence of some structural disorder. NMR spectra of the hexanol and ethanol samples (Figure 2) are qualitatively similar and are dominated by an intense resonance with a large hyperfine shift (780 ppm for the ethanol sample vs 720 ppm for the hexanol sample), assigned to octahedral Li ions in between the Mn layers, and a pronounced shoulder to lower frequencies. The difference in shifts for the two samples may be due to a slightly different average oxidation state for the manganese in the two samples. Materials prepared by ion exchange under reflux in ethanol have a higher Mn oxidation state than those prepared under reflux at higher temperatures (Table 1).[8] The shoulder is ascribed to the presence of tetrahedral sites within the layers and/or a distribution in oxidation states; tetrahedral ions, and Li ions near higher numbers of Mn^{3+} ions generally resonating at lower frequencies. The shoulder is more pronounced for the hexanol sample, and an additional weaker resonance at 512 ppm is observed, which is ascribed to the presence of spinel-like local environments in the sample. This suggests that the

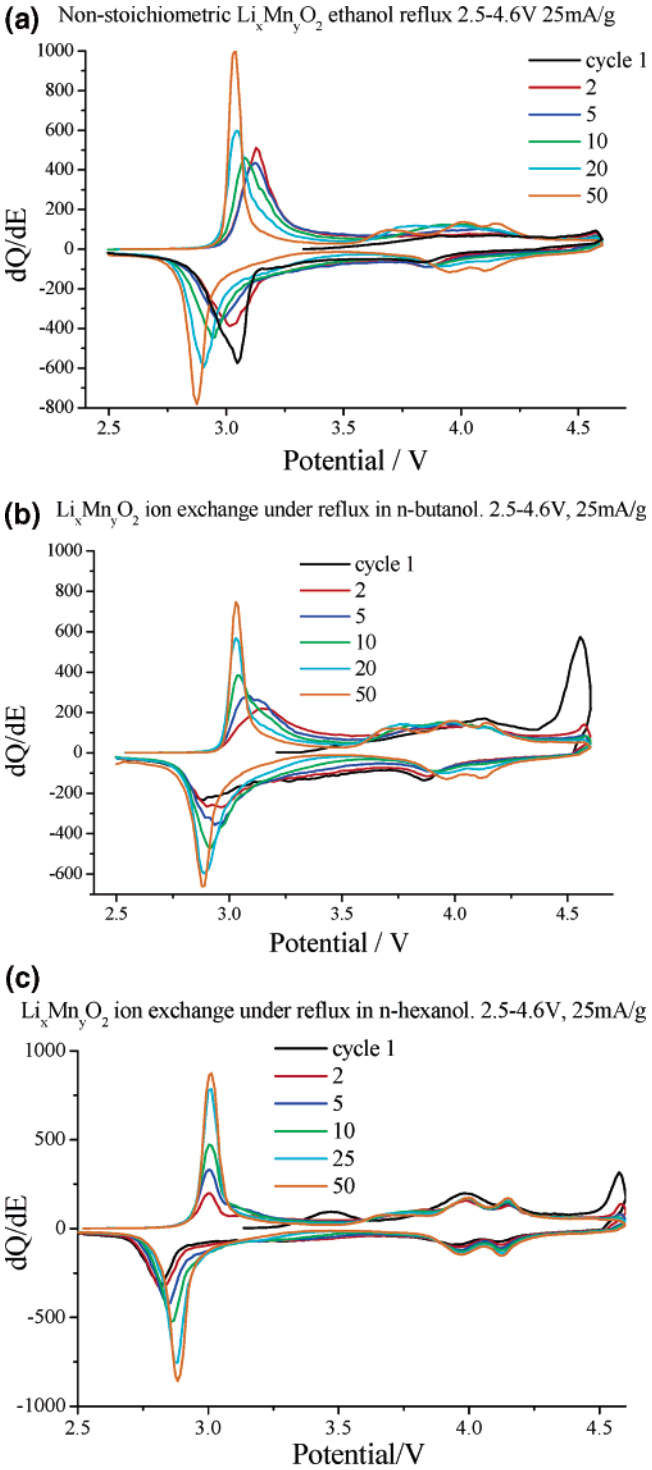

Figure 3. Incremental capacity plots for nonstoichiometric layered $Li_xMn_yO_2$ as a function of cycle number. Materials were prepared by ion exchange with excess LiBr under reflux in (a) ethanol, (b) *n*-butanol, and (c) *n*-hexanol. Cycling was performed at 25 $mA \cdot g^{-1}$ (approximately *C*/8). Voltage limits = 2.5−4.6 V. T = 30 °C.

higher temperature of the ion exchange performed in *n*-hexanol (~160 °C) induces some spinel formation. Weaker resonances are also seen at approximately 580, 350, and 140 ppm for the hexanol sample. Resonances at approximately 580 ppm were assigned, in our previous study, to local environments within an intermediate structure, which contains Li in tetrahedral sites in spinel-like regions, or in the Li−Mn dumbbells formed within the layered phase; again this suggests that the transformation to spinel has been

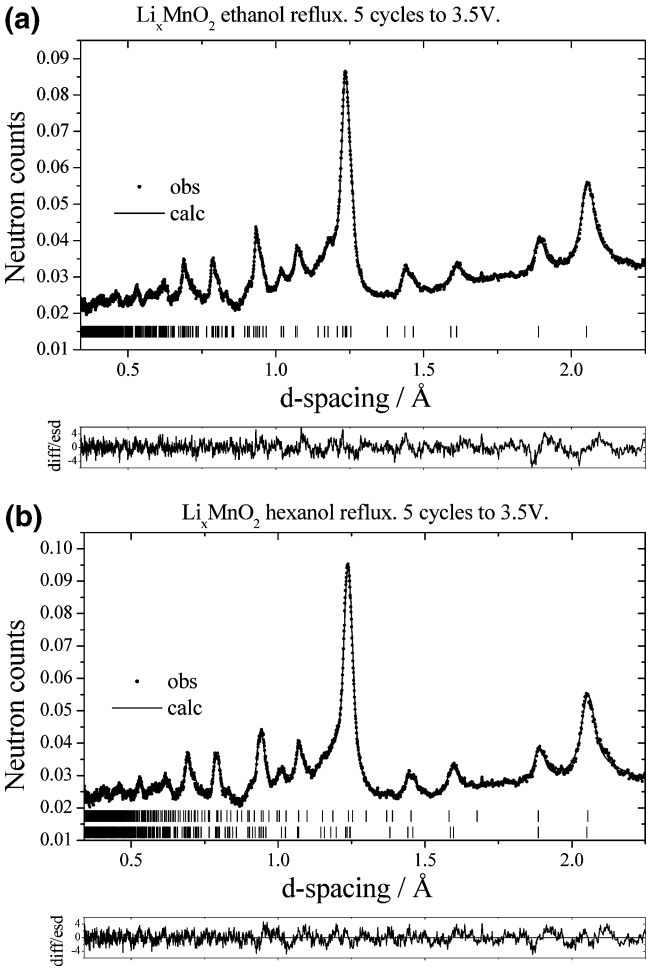

Figure 4. Refined powder neutron diffraction pattern using a splayered model for nonstoichiometric layered $Li_xMn_yO_2$ stopped at 3.5 V on the fifth discharge. (●) Observed data; (—) calculated pattern. The lower line is the difference/esd. (a) Prepared by ion exchange under reflux in ethanol; (b) prepared by ion exchange under reflux in *n*-hexanol. Upper tick marks represent allowed spinel reflections; lower tick marks represent allowed layered reflections.

initiated by the higher temperature ion-exchange process. The resonance at 350 ppm is probably due to Li near higher fractions of Mn^{3+} ions. A resonance with a similar hyperfine shift has been observed during the reduction of ramsdellite for a material with a lithium content $Li_{0.5}MnO_2$[22] and in the Li spectrum of *O*2-$Li_yCu_{0.11}Mn_{0.89}O_{2.05}$, where it was assigned to the tetrahedral (*T*2) sites.[23] It is therefore possible that this resonance is due to Li in the splayered (tetrahedral) sites near Mn^{3+}, since this local environment is expected to resonate at a lower frequency than the tetrahedral environment found in $LiMn_2O_4$, due to the smaller number of Li−O−Mn contacts (9 vs 12 for the splayered vs spinel environments, respectively).[1] The very weak resonance at approximately 140 ppm is assigned to Li in Mn^{3+}-rich regions, since layered $LiMnO_2$ resonates at a similar frequency (approximately 145 ppm).[24] The observation of the 380 and 140 ppm resonances in the hexanol sample and not in the ethanol sample is consistent with the lower average oxidation state for Mn in the former material.

(22) Paik, Y. Ph.D. Thesis, SUNY Stony Brook, 2004.
(23) Eriksson, T. A.; Lee, Y. J.; Hollingsworth, J.; Reimer, J. A.; Cairns, E. J.; Zhang, X.-f.; Doeff, M. M. *Chem. Mater.* **2003**, *15*, 4456.
(24) Lee, Y. J.; Grey, C. P. *Chem. Mater.* **2000**, *12*, 3611.

Table 2. Refined Crystallographic Parameters for $Li_xMn_yO_2$ Stopped at 3.5 V on Fifth Discharge

atom	Wyckoff symbol	*x*/*a*	*y*/*b*	*z*/*c*	B_{iso}	occupancy
(a) Ethanol Reflux, Splayered Model[a]						
Li1	3b	0.0	0.0	0.5	0.6(2)	0.56(3)
Li2	6c	0.0	0.0	0.125(3)	0.5(−)	0.11(1)
Mn	3a	0.0	0.0	0.0	0.75(10)	0.85(2)
O1	6c	0.0	0.0	0.2608(1)	1.05(4)	1
(b) *n*-Hexanol Reflux, Splayered + Spinel Model[b]						
Li	3b	0.0	0.0	0.5	1.2(4)	0.89(5)
Li2	6c	0.0	0.0	0.124(6)	0.5(−)	0.09(2)
Mn	3a	0.0	0.0	0.0	0.12(14)	0.76(2)
O1	6c	0.0	0.0	0.2610(2)	1.44(10)	1

[a] $R_e = 1.51\%$, $R_{wp} = 2.24\%$, and $R_p = 1.85\%$; $a = 2.8724(7)$ Å and $c = 14.495(3)$ Å. [b] $R_e = 1.94\%$, $R_{wp} = 2.91\%$, and $R_p = 2.46\%$. Phase ratio of splayered:spinel was 80(1)%:20(1)% (by volume). Parameters for splayered phase: $a = 2.8752(12)$ Å and $c = 14.391(5)$ Å. Spinel phase $a = 8.240$ Å; atomic and lattice parameters were not varied due to the small quantity of phase present.

The incremental capacity plots collected upon cycling cells containing various $Li_xMn_yO_2$ electrodes at 25 $mA \cdot g^{-1}$ and between potential limits of 2.5 and 4.6 V versus Li^+ (1 M)/Li are shown in Figure 3. We will denote samples prepared by ion exchange with excess LiBr under reflux in ethanol as eth, butanol as but, and *n*-hexanol as hex. A sample stopped on the fifth discharge will be denoted 5, such that a material prepared by ion exchange with excess LiBr under reflux in ethanol and stopped on the fifth discharge at 3.5 V is denoted eth5.

Five Cycles. Neutron powder diffraction data were collected for materials prepared by ion exchange with excess LiBr under reflux in ethanol and *n*-hexanol stopped at 3.5 V on the fifth discharge. In the former case (eth5) the structure is clearly still layered at this point ($R_{wp} = 2.30\%$). However, a better fit was obtained, together with more sensible refined occupancies, for a "splayered" model containing tetrahedral lithium ($R_{wp} = 2.24\%$) (Figure 4a and Table 2a). The ^{6}Li NMR spectrum of eth5 contains a broad resonance and no sharp resonance at around 510 ppm, characteristic of spinel, is observed (Figure 5). The broad resonance clearly contains several resonances, which are ascribed to Li in both octahedral and tetrahedral sites. This is consistent with the proposed splayered structural model. The incremental capacity plots for this material give no indication of the characteristic double 4 V process of spinel at this stage.

By contrast, both the structure refinements and incremental capacity plots for the *n*-hexanol material (hex5) show evidence for two phases, layered (or splayered) and spinel, in the approximate ratio 80:20 (Figure 4b and Table 2b). However, it should be noted that the incremental capacity plots for this system show the presence of the double 4 V process even on the first cycle (Figure 3c), consistent with the ^{6}Li MAS NMR of the pristine material, Figure 2.

The ^{6}Li NMR spectra for materials prepared in *n*-hexanol as a function of cycle number are shown in Figure 6. All exhibit a sharp resonance at 520−512 ppm that can be assigned to Li ions in a spinel structure. The shape of the spectrum after one cycle (charge to 4.6 V and discharge to 3.5 V) already looks completely different from the starting material and is reminiscent of what was observed for stoichiometric $LiMnO_2$ following cycling for more than two

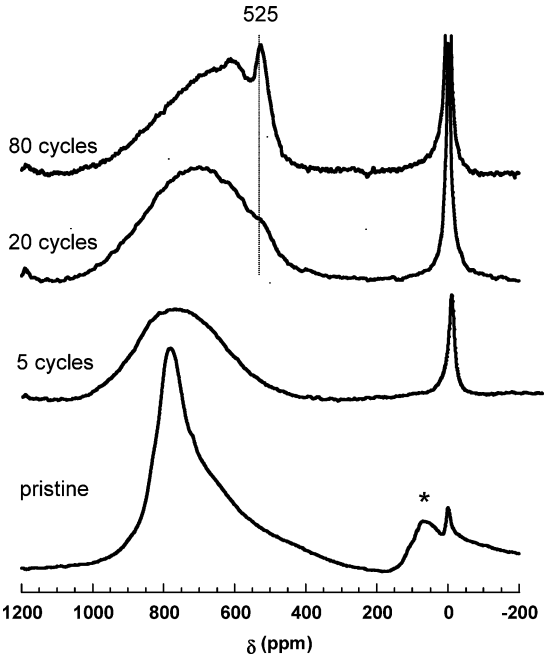

Figure 5. ^{6}Li NMR spectra of nonstoichiometric layered $Li_xMn_yO_2$ prepared by ion exchange under reflux in ethanol as a function of cycle number. The intense resonance at 0 ppm is due to lithium salts in the electrolyte.

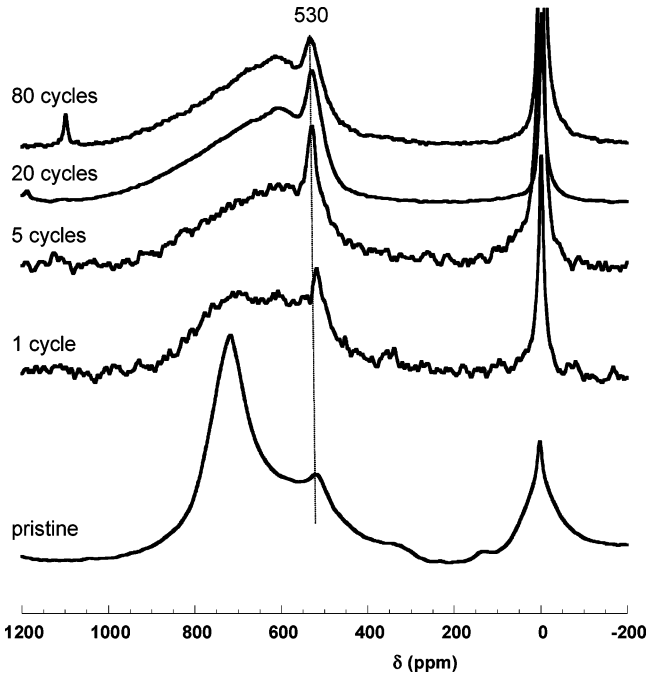

Figure 6. ^{6}Li NMR spectra of nonstoichiometric layered $Li_xMn_yO_2$ prepared by ion exchange under reflux in *n*-hexanol as a function of cycle number.

cycles.[1] Although the resolution is poor, at least three environments are resolved. The large and broad signal between 650 and 800 ppm, which probably contains several local environments, is attributed to the layered material (and accounts for approximately 60% of the signal).[1] The narrow signal at 520 ppm is from the spinel phase (12−15%). A third resonance at 550−600 ppm is assigned to the intermediate local environment. No significant change is seen between this spectrum and that following the second cycle; however, following five cycles, a clear decrease in the high-frequency resonance assigned to the layered phase is seen along with an increase in the resonance assigned to the spinel

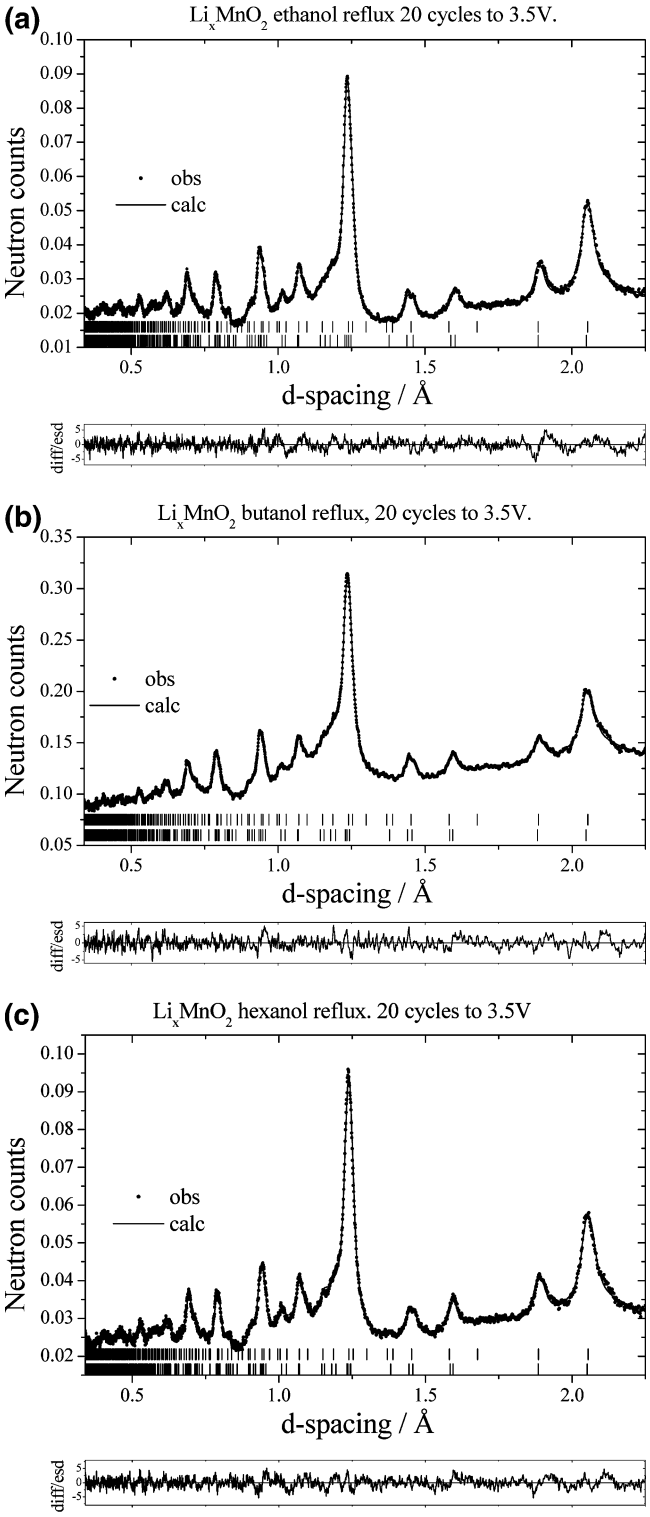

Figure 7. Refined powder neutron diffraction patterns for materials prepared by ion exchange with excess LiBr under reflux in (a) ethanol, (b) *n*-butanol, and (c) *n*-hexanol stopped at 3.5 V on the 20th discharge. In each case the model contains splayered (lower tick marks) + spinel (upper tick marks) structures.

phase. Deconvolution gives the following intensity ratios: layered (650−900 ppm) approximately 50%, spinel 20%, and intermediate environments 30%. The results are consistent with the 20% spinel found from neutron refinements.

Material prepared by ion exchange under reflux in *n*-butanol and stopped on the 10th discharge at 3.5 V exhibited intermediate behavior. There is some evidence from neutron diffraction for the presence of spinel at a concentration of around 10%.

Table 3. Refined Crystallographic Parameters for $Li_xMn_yO_2$ Stopped at 3.5 V on 20th Discharge

atom	Wyckoff symbol	*x*/*a*	*y*/*b*	*z*/*c*	B_{iso}	occupancy
(a) Ethanol Reflux, Splayered + Spinel Model[a]						
Li1	3b	0.0	0.0	0.5	1.0(3)	0.60(3)
Li2	6c	0.0	0.0	0.123(3)	0.5(−)	0.10(1)
Mn	3a	0.0	0.0	0.0	0.48(10)	0.81(2)
O1	6c	0.0	0.0	0.2608(1)	1.17(5)	1
(b) *n*-Butanol Reflux, Splayered + Spinel Model[b]						
Li	3b	0.0	0.0	0.5	0.9(3)	0.78(4)
Li2	6c	0.0	0.0	0.093(4)	0.5(−)	0.09(2)
Mn	3a	0.0	0.0	0.0	0.61(16)	0.79(2)
O1	6c	0.0	0.0	0.2607(1)	1.12(6)	1
(c) *n*-Hexanol Reflux, Splayered + Spinel Model[c]						
Li	3b	0.0	0.0	0.5	1.0(−)	0.76(4)
Li2	6c	0.0	0.0	0.132(5)	0.5(−)	0.10(2)
Mn	3a	0.0	0.0	0.0	0.13(12)	0.74(2)
O1	6c	0.0	0.0	0.2613(2)	1.48(10)	1

[a] $R_e = 1.79\%$, $R_{wp} = 2.77\%$, and $R_p = 2.31\%$. Phase ratio of splayered:spinel was 95(1)%:5(1)% (by volume). Parameters for splayered phase: $a = 2.8752(8)$ Å and $c = 14.425(3)$ Å. Spinel phase $a = 8.240$ Å; atomic and lattice parameters were not varied due to the small quantity of phase present. [b] $R_e = 1.04\%$, $R_{wp} = 1.57\%$, and $R_p = 1.33\%$. Phase ratio of layered:spinel was 86(1)%:14(1)% (by volume). Parameters for splayered phase: $a = 2.8756(10)$ Å and $c = 14.332(4)$ Å. Spinel phase $a = 8.240$ Å; atomic and lattice parameters were not varied due to the small quantity of phase present. [c] $R_e = 1.64\%$, $R_{wp} = 2.62\%$, and $R_p = 2.20\%$. Phase ratio of layered:spinel was 79(1)%:21(1)% (by volume). Parameters for splayered phase: $a = 2.880(2)$ Å and $c = 14.347(5)$ Å. Spinel phase $a = 8.240$ Å.

Twenty Cycles. Neutron powder diffraction data were collected on samples of materials prepared by all three ion-exchange routes stopped at 3.5 V on the 20th discharge. In all cases a better fit to the data was obtained by use of a two-phase model as opposed to a single layered or splayered phase (Figure 7, Table 3). However, in the ethanol case (eth20) this improvement was only marginal (χ^2 of 2.40 as opposed to 2.42). The ratios of splayered:spinel phase for the three samples were 95:5 (ethanol), 86:14 (butanol), and 79:21 (hexanol). It is interesting to note the relatively small increase in the spinel fraction in the butanol and hexanol systems compared with lower cycle numbers. The ^{6}Li NMR spectrum for the hex20 sample confirms this slow growth in the spinel fraction compared with the pristine material, with only a modest increase in intensity for the 515 ppm spinel peak (Figure 6). In the case of the eth20 sample, a shoulder at 525 ppm, which can be attributed to the spinel phase, begins to appear (Figure 5). Deconvolution of the signal gives approximately 8% spinel, consistent with the neutron refinement, considering the poor signal-to-noise ratio of our NMR spectra and the fact that NMR spectroscopy will detect signals from very small crystallites.

One Hundred Cycles. Data were obtained from both ethanol and *n*-hexanol compounds stopped at 3.5 V on the 100th discharge. The eth100 sample shows a clear increase in the proportion of spinel to 25% but appears to remain predominantly layered. In support of this proposal, a single phase refinement in a splayered model gives a significantly better fit than refinement as a spinel. The data from the hex100 sample exhibited rather poor crystallinity, which prevented a successful two-phase refinement from being

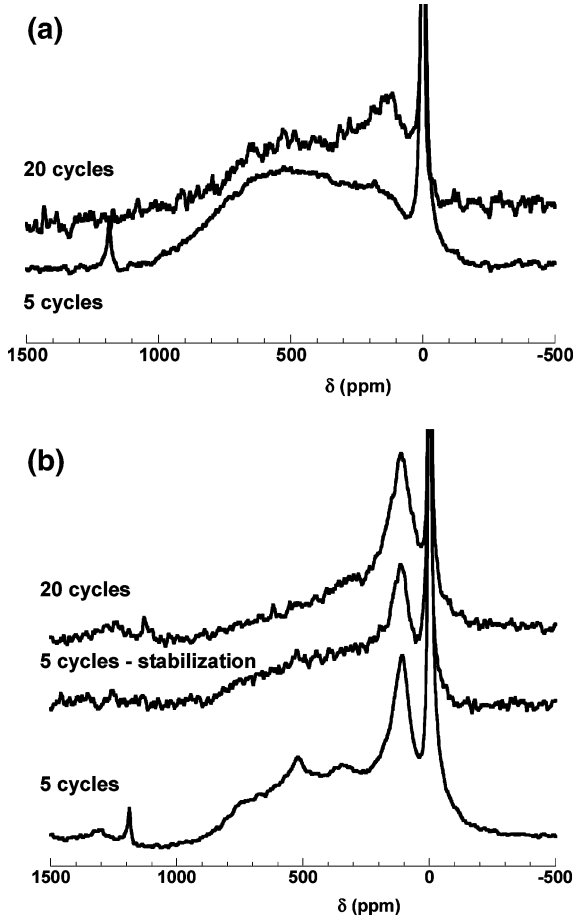

Figure 8. ^{6}Li NMR spectra of nonstoichiometric layered $Li_xMn_yO_2$ prepared by ion exchange under reflux in (a) ethanol and (b) *n*-hexanol as a function of cycle number; the cells were disassembled following discharging to 2.5 V. The sample denoted 5 cycles-stabilization was obtained after a floating step at 2.5 V of 1 week.

carried out. Again, a better single phase fit was obtained in a splayered model than as a spinel.

The NMR spectrum of a hex80 sample yields ratios similar to those obtained from the hex20 compound (23% spinel, the same as after 20 cycles within experimental error) and looks similar to that after 20 cycles. In the case of an eth80 sample, the spinel resonance at 528 ppm can clearly be seen (Figure 6) and a deconvolution gives 20% of spinel, supporting the neutron refinement (75% splayered/25% spinel) for eth100. A resonance at 610 ppm is more clearly resolved, which is ascribed to an intermediate environment (22% from deconvolution).

Local Environments on Reduction to 2.5 V. In order to assess how ordered the residual layered phases were following cycling, we also examined materials that had been discharged to 2.5 V, more ordered phases, or phases with larger grain sizes generally undergoing cooperative Jahn−Teller distortions of the particles on reduction of more than 50% of the manganese ions to Mn^{3+}; layered Mn^{3+} materials are associated with very distinct NMR signals at approximately 135−145 ppm, while spinel phases ($Li_2Mn_2O_4$) resonate at approximately 100 ppm.[11] For the hexanol sample, an intense broad resonance is observed at approximately 112 ppm even following 20 cycles, along with resonances spanning a range of 200−800 ppm, which are assigned to Li near Mn^{3+} (and residual Mn^{4+} ions) in less crystalline, (higher oxidation state) phases or regions of the sample (Figure 8b). In contrast, only a very weak resonance is seen at approximately 120 ppm in the ethanol sample following 5 and 20 cycles (Figure 8a). These results should be contrasted with the results for the stoichiometric materials, where a resonance at 135 ppm dominated the spectrum of a sample discharged to 2.5 V following 5 cycles, with the resonance gradually decreasing in intensity upon cycling, essentially disappearing by approximately 35 cycles, with resonances at 530 ppm and above dominating the spectrum. Even though spinel phases were formed upon extended cycling, the small grain sizes of the particles, or the residual defects in the samples, prevented the Jahn−Teller distortion from occurring. Thus, the ethanol sample appears to be noticeably more disordered than the hexanol sample so that the majority of the original layered phase does not undergo a Jahn−Teller distortion in the first few cycles.

Discussion

The layered and spinel structures are compared in Figure 9, with each presented with the close-packed oxygen layers in the same orientation. We know that transformation to a spinel structure ultimately occurs upon cycling, and this must involve 25% of the Mn ions migrating from the octahedral sites in the transition metal layers into octahedral sites in the Li layers, with the Li ions in these layers being displaced to tetrahedral sites.

We discussed the mechanism of such a migration in our previous paper on stoichiometric layered $LiMnO_2$ and summarize it here. Within the Mn layers, the MnO_6 octahedra share faces with bridging empty tetrahedral sites. Similarly, within the Li layers, empty tetrahedral sites share faces with LiO_6 octahedra. Furthermore, the MnO_6 octahedra share faces with empty tetrahedral sites in the LiO_6 layers immediately above and below the Mn layers. Again the corresponding situation occurs for the LiO_6 octahedra. Mn ions can easily migrate through a common face into the empty tetrahedral sites in the Li layers once there are sufficient Li vacancies, since the remaining lithium ions can readily avoid the three octahedral sites that share faces with the now-occupied tetrahedral site. Following this Mn displacement, there is now a vacant Mn site and it is possible to displace a Li ion from its octahedral site through a shared face into a neighboring tetrahedral site in the Li layer since there is no longer an unfavorable face sharing interaction with a Mn ion.

Reed et al.[17] have investigated the layered to spinel transformation using computational methods (density functional theory).[17] They proposed a two-stage process in which the first stage involves displacement of a Mn ion from an octahedral to a tetrahedral site in the neighboring lithium layer, with a lithium ion in the other adjacent layer migrating from an octahedral site into the tetrahedral site that shares a face with the now-vacant Mn site, as described above. As a consequence, each pair of tetrahedral Li and Mn ions form a "dumbbell" with the empty octahedral Mn site between them. A structure with such an arrangement has been referred to as splayered. Following this first stage, a further correlated rearrangement of Li and Mn ions is thought to occur in order to form the spinel structure. Reed et al. have shown that the

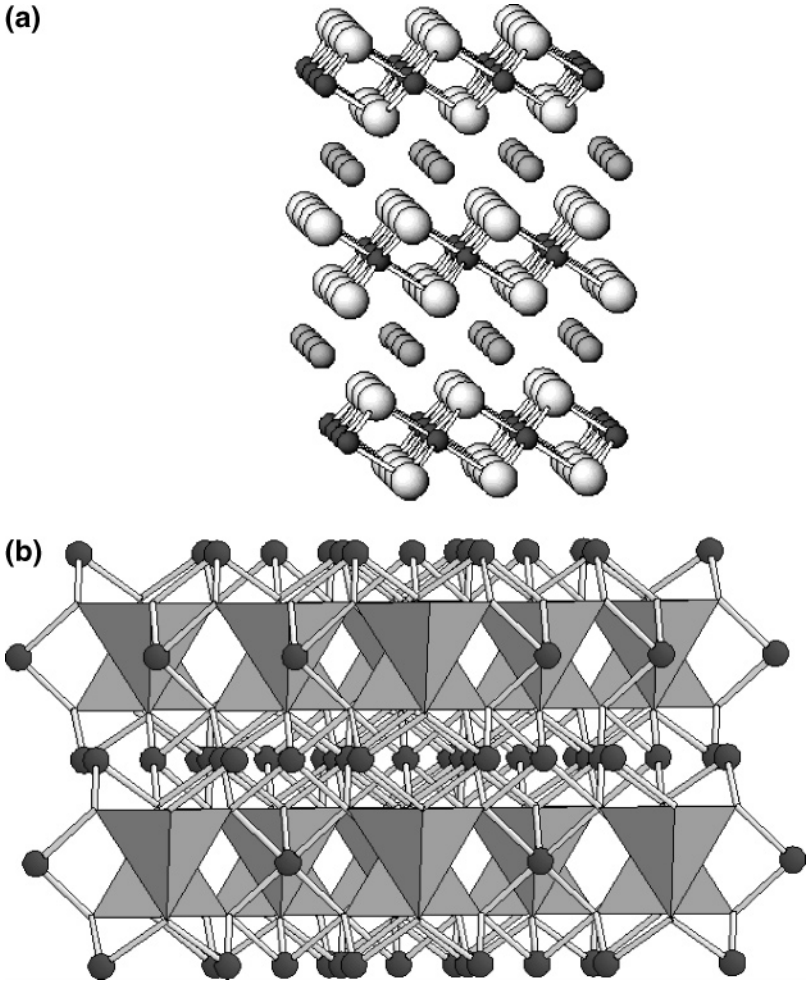

Figure 9. (a) View of layered $LiMnO_2$ structure. Dark gray,− Mn; gray, Li; white,− O. (b) View of $LiMn_2O_4$ spinel structure emphasising layers. Dark gray,− Mn; gray, tetrahedral cation sites.

first process is relatively facile whereas the second, involving the nucleation and growth of spinel, is more energetically demanding.[17]

This process occurs in all materials, irrespective of the ion-exchange route. However, it is apparent that the high temperature of the ion exchange under reflux in *n*-hexanol is sufficient to promote formation of some spinel within the as-synthesized material. In the first 50 or so cycles, the various layered $Li_xMn_yO_2$ compounds behave rather differently, with a higher spinel fraction observed for materials ion-exchanged under more extreme conditions. However, to some extent this reflects the proportion of spinel present in the as-prepared phase. Upon cycling, all the different layered $Li_xMn_yO_2$ compounds start to transform to a long-range ordered spinel and this is evident in the diffraction and NMR data. However, the rate of this transformation is significantly slower than was observed in stoichiometric layered $LiMnO_2$ with only 25% spinel observed after 100 cycles. X-ray diffraction and electrochemical data obtained after 200 cycles show that the structure continues to evolve. Ultimately, upon extended cycling the entire structure will transform to an ordered spinel phase. The NMR data collected following discharging to 2.5 V demonstrate that the ethanol phase is more disordered from the start so that a cooperative Jahn−Teller distortion does not occur in the fully reduced samples, at least in intermediate charge cycles investigated. The hexanol phase, despite containing a higher spinel fraction, appears to contain a more ordered layered structure initially, and consequently a Jahn−Teller distortion is observed following discharging to 2.5 V.

Acknowledgment. P.G.B. thanks the Royal Society and EPSRC for funding. C.P.G. thanks the National Science Foundation for support via Grants DMR0211353 and DMR0506120.

CM0621747